



Published in final edited form as:

Bioorg Med Chem. 2015 April 15; 23(8): 1849–1857. doi:10.1016/j.bmc.2015.02.022.

Preparation and biological evaluation of synthetic and polymer-encapsulated congeners of the antitumor agent pactamycin: Insight into functional group effects and biological activity

Robert J. Sharpe^a, Justin T. Malinowski^a, Federico Sorana^a, J. Christopher Luft^{a,b}, Charles J. Bowerman^a, Joseph M. DeSimone^{a,b,c,d,e,f,g,h}, and Jeffrey S. Johnson^{a,*}

^aDepartment of Chemistry, University of North Carolina at Chapel Hill, Chapel Hill, NC 27599-3290, United States

^bDepartment of Molecular Pharmaceutics, Eshelman School of Pharmacy, University of North Carolina at Chapel Hill, Chapel Hill, NC 27599-3290, United States

^cLineberger Comprehensive Cancer Center, University of North Carolina at Chapel Hill, Chapel Hill, NC 27599-3290, United States

^dDepartment of Chemical and Biomolecular Engineering, North Carolina State University, Raleigh, NC 27695-8613, United States

^eCarolina Center of Cancer Nanotechnology Excellence, University of North Carolina at Chapel Hill, Chapel Hill, NC 27599-3290, United States

^fInstitute for Nanomedicine, University of North Carolina at Chapel Hill, Chapel Hill, NC 27599-3290, United States

^gInstitute for Advanced Materials, University of North Carolina at Chapel Hill, Chapel Hill, NC 27599-3290, United States

^hSloan-Kettering Institute for Cancer Research, Memorial Sloan-Kettering Cancer Center, New York, NY 10065-9321, United States

Abstract

The synthesis and biological analysis of a number of novel congeners of the aminocyclopentitol pactamycin is described. Specific attention was paid to the preparation of derivatives at crucial synthetic branch points of the parent structure, and biological assays revealed a number of insights into the source of pactamycin's biological activity. Additionally, the encapsulation of pactamycin and select derivatives into the PRINT[®] nanoparticle technology was investigated as a proof-of-concept, and evidence of bioactivity modulation through nanoparticle delivery is demonstrated. This work has provided heretofore unrealized access to a large number of novel compounds for further evaluation.

© 2015 Elsevier Ltd. All rights reserved.

*Corresponding author. Tel.: +1 9198434936. jsj@unc.edu (J.S. Johnson).

Supplementary data

Supplementary data associated with this article can be found, in the online version, at <http://dx.doi.org/10.1016/j.bmc.2015.02.022>.

Keywords

Pactamycin; Nanoparticles; Structure activity relationships; Structural derivatization

1. Introduction

Pharmaceutical development through organic synthesis remains a critical feature of the drug discovery process.¹ Upon identification of an initial hit via high-throughput screening, a significant amount of structural modification is often required before a lead candidate can be advanced to clinical trials. Natural molecules are often identified as initial hits in these screenings; however, later modification of their complex structures toward the preparation of useful drug molecules can be hindered by the deficiency of a practical and flexible chemical synthesis.² As a result, the continued advancement of synthetic organic methodology is critical for facile and flexible drug discovery and development.

Pactamycin (**1**, Fig. 1) is an example of a valuable natural target that has yet to reach its full medicinal potential, at least in part due to its structural complexity. Isolated in 1961 from a fermentation broth of *Streptomyces pactum* var. *pactum* by scientists at the former Upjohn Chemical Co.,³ pactamycin represents the most complex aminocyclitol antibiotic ever discovered. Researchers at Upjohn showed it to be active against Gram-positive and Gram-negative bacteria as well as against a number of cancer cell lines in vitro.⁴ More recent biological studies have demonstrated pactamycin to have potent antiviral (complete inhibition of polio-infected HeLa cells at 10^{-7} M) and antiprotozoal qualities (P.f. K1: IC₅₀ = 14.2 nM).^{5,4b} Unfortunately, this promising biological profile is hindered by pactamycin's high cytotoxicity against human eukaryotic cell lines (MRC-5: IC₅₀ = 95 nM).^{5,4b} X-ray crystallographic studies have shown that the source of this activity stems from pactamycin's ability to bind to the 30S ribosomal subunit acting as an RNA dinucleotide mimic.⁶ A complex array of H-bonding interactions within the 30S site enables pactamycin to act as a universal inhibitor of translocation. Its impressive biology has attracted the attention of a multidisciplinary field in hopes of transforming pactamycin into a suitable therapeutic (Fig. 1).

In addition to **1**, a number of naturally-occurring structural congeners have been isolated from related *Streptomyces* bacteria, displaying varied bioactivities. 7-Deoxypactamycin (**2**) and jogyamycin (**3**) have shown increased antiprotozoal activity relative to **1**.⁷ A third natural analog, pactamycate (**4**), has also been reported.⁸ Alternatively, biosynthetic engineering studies pioneered by Mahmud and co-workers have provided researchers with the first series of unnatural structural analogs such as TM-025F (**5**) and TM-026F (**6**), which display comparable activities to pactamycin against *Plasmodium falciparum*.^{8b,9} These data have renewed promise for pactamycin analogs in drug development.

Moreover, encapsulation of natural cytotoxic agents into nanoparticles (NPs) has also shown improved clinical benefits, the most germane of these being reduction of undesired toxic side effects and increased therapeutic delivery to the target of interest. This approach has been successfully implemented in the case of doxorubicin (Doxil[®]),¹⁰ paclitaxel (Abraxane[®])¹¹ and others.¹² More recently, Bind Therapeutics¹³ and Cerulean¹⁴ have

ongoing clinical trials in NP formulations of cancer therapeutics (docetaxel, irinotecan, and camptothecin). DeSimone and co-workers have demonstrated the use of the Particle Replication in Non-Wetting Templates (PRINT[®]) technology to modulate the activity of cytotoxic agents such as docetaxel, reducing unwanted side-effects and increasing therapeutic activity in vivo.¹⁵ To the best of our knowledge, however, the incorporation of pactamycin or its congeners into NPs of any type with the goal of bioactivity attenuation has not yet been explored.

While an efficient chemical synthesis of **1** might provide the most flexibility in structural derivatization, the inherent complexity of the molecule has rendered this a difficult undertaking. The heavily-compacted and heteroatom-rich functionality in pactamycin presents a number of challenges toward selective structural modification. Additionally, while the unique functional groups present in the molecule (salicylate, dimethylurea, aniline) offer novel branch points for structural diversification, methods with which to install these moieties are underexplored in the literature.¹⁶ To these aims, a number of synthetic studies have been reported by Isobe, Knapp, Looper, Nishikawa, and our group in the past decade.¹⁷ In 2011, Hanessian and co-workers described the first total synthesis of pactamycin in 32 steps from L-threonine, enabling previously unrealized access to synthetic congeners.¹⁸ Since this initial publication, Hanessian has demonstrated the efficacy of his route to deliver pactamycin derivatives at the C1-dimethylurea and the C3 aniline positions such as compounds **7** and **8**.¹⁹

Our group began work on the total synthesis of **1** in 2009, and this work culminated in 2013 with a 15-step, asymmetric synthesis from commercially available 2,4-pentanedione (Fig. 2).²⁰ Critical to our approach was to assemble the molecule in a fashion such that key functional groups were installed both in their native form and in a late-stage fashion; we surmised that this approach would provide the greatest possible flexibility, facilitating investigations of structure-activity relationships at all critical branch points. To this end, we envisaged a synthon such as **9** in which exploitation of appropriate functional handles at the correct stage would install the requisite functionalities.

A summary of our disclosed synthesis endgame is described in Figure 3, wherein ketone intermediate **10** (synthesized in ten steps from 2,4-pentanedione in gram quantities) would serve as our first point of derivatization.²⁰ Nucleophilic methylation of **10** proceeded in good yield to provide carbinol **11** in 75% yield of a single diastereomer at C5. Sc(OTf)₃-promoted addition of *m*-acetylaniline installed the substituted C3-aniline necessary for elaboration to **1**, upon which silyl deprotection afforded tetraol **12**. Introduction of the remaining salicylate moiety to the C6-hydroxymethylene of **12** was accomplished via reaction with the previously reported acyl electrophile **13**, which upon hydrogenative removal of the Cbz protecting group delivered pactamycin in 15 steps and 1.9% overall yield. With this strategy established, we shifted our focus to examining the route's flexibility toward analog preparation.

Herein, we delineate our efforts in the synthesis and biological evaluation of novel pactamycin congeners. Additionally, we report the first studies incorporating pactamycin

and select derivatives into polymeric NPs, fabricated using the PRINT[®] technology, with the goal of enhancing activity and selectivity while mitigating unwanted toxicities.

2. Results and discussion

2.1. C3-aniline

We first pursued the preparation of pactamycin congeners at the C3-aniline position, inspired by a related epoxide-opening strategy by Hanessian and co-workers (Table 1).^{18,19} We were encouraged by the aniline flexibility demonstrated by Hanessian in their earlier report and hoped that epoxide **11** would participate in related transformations with functionally and electronically diverse anilines.

Indeed, we were pleased to find that epoxide **11** reacted readily in the presence of a number of substituted anilines in moderate to excellent yields, providing anilines **14a–h**. Notably, while the installation of *m*-acetylaniline to **11** necessitated superstoichiometric amounts of Sc(OTf)₃, all subsequent anilines examined in the reaction proceeded to completion using 50 mol % Sc(OTf)₃. We suspect that this is an outgrowth of both low nucleophilicity and poor solubility of the parent *m*-acetylaniline under the reaction conditions. With the aniline tolerance established, we turned our attention to alternative nitrogen nucleophiles. Unfortunately, all non-aromatic nitrogen sources (RNH₂, R₂NH, ⁻N₃) failed to react with **11**, giving either no reaction or starting material decomposition. Addition products **14a–h** were carried through the endgame sequence described previously, delivering derivatives **15a–h** (Fig. 4). In the case of addition product **14g**, the aryl bromide was reduced during hydrogenolysis, delivering α -naphthyl anilide **15g**.

2.2. C1-dimethylurea

Hanessian's approach toward preparation of pactamycin analogs at the C1 dimethylurea position substituent relied on the trapping of an in situ generated isocyanate electrophile late in the synthesis.¹⁸ This tactic proved effective in the preparation of a series of functionalized ureas in good yields.¹⁹ By contrast, our synthesis of **1** utilized an early-stage N–H insertion reaction to install the urea.²⁰ Synthetic diversification from this early intermediate would be a significant challenge. Consequently, we envisaged a similar isocyanate formation/trapping strategy from carbinol intermediate **11** via the acid-catalyzed elimination of dimethylamine (Fig. 6).

After some experimentation, treatment of **11** with NH₄Cl in H₂O and MeOH resulted in complete elimination of dimethylamine and convergence to a single product. However, ¹H NMR analysis revealed that the intermediate isocyanate had undergone intramolecular ring closure with the C2-carbamate to furnish imidazolidinone **17** in 73% yield. Although this result rendered our intermolecular isocyanate trapping strategy unfeasible, we postulated that this reactivity might be exploited toward analog preparation of the naturally-occurring congener pactamycate **4** (Fig. 5).

Selective deprotection of the C7-TBS ether in **16** with oxone furnished the corresponding secondary alcohol **18** in 84% yield, which we postulated would serve as a more nucleophilic trapping agent for the intermediate isocyanate. Indeed, upon treatment of **18** with NH₄Cl in

H₂O/MeOH, the in situ generated isocyanate underwent trapping by the unprotected C7 hydroxyl to afford oxazolidinone **19** in 73% yield. Removal of the TBDPS protecting group with TBAF provided triol **20**, which upon Cbz deprotection, afforded De-6-MSA pactamycate **21**, which has been previously characterized.^{18b} This result confirmed that the intermediate isocyanate generated from **18** had indeed been engaged by the C7 hydroxyl (and not the C2 carbamate). With this route established, we resolved to prepare a subset of varied C3 pactamycate structures. Beginning with anilides **14b**, **14c**, and **14e** already in hand from the C3 derivatization studies, TBS deprotection followed by oxazolidinone formation gave the corresponding diols, which upon desilylation, acylation and hydrogenolysis, provided pactamycate derivatives **22a–c**.

2.3. C5-tertiary alcohol

We next began examining reactivity of the ketone in **10** with the goal of diversification at C5 (Table 2). To this end, we were pleased to find this ketone reacted readily with ethyl, ⁿhexyl, and vinyl magnesium bromide to give the corresponding carbinols in good yields. Unfortunately, when larger alkyl (entries 4, 5 and 8) and aryl nucleophiles (entries 6 and 7) were examined, we observed only un-productive side reactions²¹ or complete starting material recovery. With this limitation established, we speculated that hydride might also be a suitable nucleophile. In the event, treatment of **10** with NaBH₄ in MeOH at –45 °C provided alcohol **23c** in good yield with analogous stereofidelity to that observed in the addition of carbon nucleophiles.

With addition products **23a–c** in hand, we proceeded in the synthesis to complete C5 analog preparation (Fig. 7). We were surprised to find, however, that subjection of these intermediates to the optimized conditions for C3 *m*-acetylaniline installation gave only significant amounts of recovered starting material. Increasing the loading of Sc(OTf)₃ or the reaction time/temperature had seemingly no effect. It seems reasonable that this addition is sluggish either due to poor coordination of the Lewis acid or by an unfavorable substrate conformation for addition relative to the parent C5-methyl compound (**11**). In order to circumvent this issue, we turned to the strategy of Hannesian and coworkers wherein the required C3 *m*-acetylaniline was incorporated via an 2-(prop-1-en-2-yl)aniline surrogate.¹⁸ The acetophenone was later revealed via oxidation. In our system, this strategy also proved effective, providing 2-(prop-1-en-2-yl)aniline anilines **24a–c** in good yields. Johnson–Lemieux oxidation of the resulting alkenes provided the desired *m*-acetylanilines **25a–c** in good yields over the three-step sequence. Completion of the remaining synthetic sequence provided C5 pactamycin derivatives **26a–c**.

2.4. C6,C7-hydroxyl

The final point of diversification centered on manipulation of the salicylate-bearing C6 ester in **1** (Table 3). Gratifyingly, efficient monoacylation of tetraol **12** was accomplished with a variety of aliphatic and aromatic acyl electrophiles in good yields (entries 1–5). The resulting monoesters were subjected to the previously employed conditions for Cbz deprotection, providing derivatives **27b–e**. However, in the case of the differentiated methoxyphenol **27a** (entry 1), only decomposition was observed upon hydrogenolysis.

Cognizant of the documented bioactivity difference across multiple cell lines observed between **1** and its 7-deoxy congener (**2**),⁷ reduction of the C7-hydroxyl to its corresponding methylene was also probed. Unfortunately, all conditions explored (from a number of different intermediates in our route) failed to deliver the desired C7-methylene. As an alternative strategy, we envisaged masking of the C7 hydroxyl via its ester might serve the same purpose (i.e., removal of the H-bonding interaction at C7).⁶ To this end, C6–C7 bis-acylated derivatives (entries 6–8) were synthesized with varying degrees of steric encumbrance. Cbz hydrogenolysis provided the diesters **27f–h**.

3. Results and discussion

3.1. Biological evaluation

Having prepared a library of novel compounds, we set out to examine their varied biological profiles. Specifically, compounds were tested against breast, ovarian, and lung *carcinoma* cell lines. Additionally, the human embryonic cell line for which pactamycin's toxicity has been established (MRC-5) was assayed for comparison.^{5,4b} The results for all derivatives are summarized in Table 4. As anticipated, pactamycin (entry 1) displayed exceptional potency, showing nanomolar inhibition against all three carcinoma cell lines. For comparison, the penultimate intermediate in our synthesis of pactamycin (**28**) bearing Cbz protection at the C2-aminomethine (entry 2) showed a dramatic decrease in activity relative to **1**. In order to better understand the effect of chirality on the parent pactamycin structure, *ent*-pactamycin (*ent*-**1**) (entry 3) was synthesized in high enantiomeric purity via a slight modification of the previously published route (see Supporting information) and assayed in our study. As illustrated in Table 4, *ent*-**1** showed a threefold order of magnitude decrease in bioactivity, illustrating the impact of the natural enantiomer of **1** to effective cell-growth inhibition.

Generally, all C3-aniline derivatives (entries 4–11) showed a marginal to significant decrease in activity relative to **1** across all cell lines, although **15b** (entry 5) showed comparable activity against A549 (EC₅₀ = 141 nM) with a marginal decrease in MRC5 activity. With regard to the pactamycate series of analogs, De-6-MSA pactamycate **21** (entry 12) showed only minor cell-growth inhibition. This was not an altogether unexpected result, however, as biological assays of **21** conducted by Hanessian and co-workers also showed little promising activity.^{19,6c} Altering the C3 aniline position of the pactamycate parent structure (entries 13–15) resulted in complete loss of biological activity. These results, in combination with those of the pactamycin C3 analogs, speak to the importance of the *m*-acetyl functionality in **1** to its bioactivity.²²

The results of compounds bearing diversity at C5 are shown in entries 16–19. In combination with the C5 derivatives previously described (vide supra), an additional derivative **29** (entry 19) was prepared bearing alternate functionality at the C3 aniline for comparison (see Supporting information). Extending the length of the carbon chain at C5 (entries 16 and 17) had significantly deleterious effects to bioactivity as a complete loss of *carcinoma* activity was observed, leaving only low inhibition of MRC-5. However, removing alkyl functionality altogether at C5 (entries 18 and 19) had the opposite effect, as these C5 protio analogs displayed the greatest activity across all cell lines of any compound

tested in our study (including pactamycin). We speculate that these results are primarily a function of adjusting the lipophilicity of the structure relative to **1**.²³

The results of our diversification of the C6 hydroxymethylene (entries 22–25) are in agreement with Hanessian's earlier findings.^{19,6c} Namely, no significant gain (or loss) of biological activity was observed when the salicylate ester was altered relative to the parent pactamycin structure. These results further support the hypothesis that the C6 ester side chain has a limited role in the key binding event of **1** in the 30S ribosome.^{19,6c} The three prepared C6,C7 bis-acylated derivatives (entries 24–26) showed a linear decrease in activity with steric encumbrance of the ester group. These results suggest that the C7 hydroxyl in **1** plays a larger role in the bioactivity of the structure than the C6 hydroxymethylene.

Upon collection of these initial data, derivatives **15f**, **26c**, **27f**, **27c**, and *ent*-(**1**) were identified as the most promising compounds and were assayed via the NCI 60 human tumor cell line screen. Upon initial one-dose screening, all five compounds were found to have sufficient activity to merit the subsequent five-dose assay. These derivatives were evaluated to determine GI₅₀ (50% growth inhibition) values. The results of these assays are summarized in Table 5. Additionally, the previously documented cell data for **1** is shown for comparison.

As expected based on our initial screen, *ent*-(**1**) showed multiple orders of magnitude loss in activity across the entire assay. By contrast, compound **26c** bearing a secondary hydroxyl at C5 demonstrated exceptional activity, showing nM inhibition throughout the screen and outperforming pactamycin in multiple cell lines. Derivatives **27c** (modified salicylate ester) and **27f** (C6, C7 diace-toxypactamycin) also demonstrated general nM activity in the assay. The final derivative **15f** bearing a fluorenyl aniline at C3 showed a general decrease in biological activity relative to **1** by factors of 10–100.

3.2. Nanoparticle fabrication-biological evaluation

With these studies completed, we set out to examine the efficacy of pactamycin and select analogs to activity modulation via nanoparticle encapsulation. Polymeric PRINT[®] nanoparticles were fabricated by encapsulating compounds **1**, **15e**, and **26c**, in poly(D,L-lactide) using previously described methods.^{15b,24} Compounds **15e** and **26c** were selected on the basis of observing the effect of nanoformulation on derivatives both more and less bioactive than **1**. PRINT NPs containing **1** and derivatives **15e** and **26c** all showed similar hydrodynamic radii and PDI as determined by dynamic light scattering (DLS).²⁵ Scanning electron microscopy (SEM) analysis confirmed uniform particle size and shape regardless of compound identity, and drug loading of each sample was found to be ~10% as determined by HPLC.²⁶ NP-encapsulated compounds **NP-1**, **NP-15e**, and **NP-26c**, were then examined in our assay, and the results are given in Table 6 where the baseline toxicity values for each compound are restated for comparison.

In vitro cytotoxicity analysis of the derivative NP formulations showed bimodal effects on therapeutic activity. In the A549 assay, nanoparticle delivery increased the cytotoxicity of the therapeutic cargo. **NP-1** demonstrated an EC₅₀ threefold more potent than pactamycin itself (52–160 nm, respectively). **NP-26c** showed a near fivefold increase in potency when

compared to the unadulterated small molecule (6.5–32 nM, respectively). Even compounds **15e**, a less active drug in comparison to **1**, showing a nominal reduction in EC₅₀ value for the A549 cell line. Of significant interest was the increase in selectivity observed for **26c**, wherein the EC₅₀ for A549 decreased while the EC₅₀ for MDA-MB-231 and MRC5 increased.

4. Conclusions

In summary, we have demonstrated the efficacy of our synthetic approach to efficient and modular preparation of a number of varied analogs of the complex aminocyclitol pactamycin. These results have provided additional insight into the roles that each functional group plays in providing the observed activity of the parent structure. Additionally, we have established a heretofore undocumented proof-of-concept for the modulation of the pactamycin structure via the use of the PRINT[®] nanoparticle delivery vehicle. A wider range of cell-based assays and the further examination of pactamycin derivatives using the PRINT technology is planned and will be reported in due course.

Supplementary Material

Refer to Web version on PubMed Central for supplementary material.

Acknowledgments

The project described was supported by Award No. R01 GM084927 from the National Institute of General Medical Sciences and by the University Cancer Research Fund. R.J.S. acknowledges an NSF Graduate Research Fellowship. R.J.S. and J.T.M. acknowledge an ACS Division of Organic Chemistry graduate fellowship. F.S. acknowledges BI Research Italia S.a.s. di BI IT S.r.l. and University of Camerino (Italy) for a doctoral fellowship. Maribel Portillo is acknowledged for experimental assistance and preparation of select derivatives.

References and notes

1. MacCoss M, Baillie TA. *Science*. 2004; 303:1810. [PubMed: 15031494]
2. Schreiber S. *Science*. 2000; 287:1964. [PubMed: 10720315]
3. Argoudelis AD, Jahnke HK, Fox JA. *Antimicrob Agents Chemother*. 1962:191.
4. (a) Bhuyan BK, Dietz A, Smith CG. *Antimicrob Agents Chemother*. 1962:184. (b) Iwatsuki M, Nishihara-Tsukashima A, Ishiyama A, Namatame M, Watanabe Y, Handasah S, Pranamuda H, Marwoto B, Matsumoto A, Takahashi Y, Otoguro K, Omura S. *J Antibiot*. 2012; 65:169. [PubMed: 22234298]
5. Taber R, Rekosh D, Baltimore D. *J Virol*. 1971; 8:395. [PubMed: 4331648]
6. (a) Dinos G, Wilson DN, Teraoka Y, Szaflarski W, Fucini P, Kalpaxis D, Nierhaus KH. *Mol Cell*. 2004; 13:113. [PubMed: 14731399] (b) Carter AP, Clemons WM Jr, Brodersen DE, Morgan-Warren RJ, Wimberly BT, Ramakrishnan V. *Nature*. 2000; 407:340. [PubMed: 11014183] (c) Tourigny DS, Fernández IS, Kelley AC, Vakiti RR, Chattopadhyay AK, Dorich S, Hanessian S, Ramakrishnan V. *J Mol Biol*. 2013; 425:3907. [PubMed: 23702293]
7. Hurley TR, Smitka TA, Wilton JH, Bunge RH, Hokanson GC, French JC. *J Antibiot*. 1986; 39:1086. [PubMed: 3759660]
8. (a) Ito T, Roongsawang N, Shirasaka N, Lu W, Flatt PM, Kasanah N, Miranda C, Mahmud T. *ChemBioChem*. 2009; 10:2253. [PubMed: 19670201] (b) Lu W, Roongsawang N, Mahmud T. *Chem Biol*. 2011; 18:425. [PubMed: 21513878]
9. Almabruk KH, Lu W, Li Y, Abugreen M, Kelly JX, Mahmud T. *Org Lett*. 2013; 15:1678. [PubMed: 23521145]

10. O'Brien MER. *Ann Oncol.* 2004; 15:440. [PubMed: 14998846]
11. Gradishar WJ, Tjulandin S, Davidson N, Shaw H, Desai N, Bhar P, Hawkins M, O'Shaughnessy J. *J Clin Oncol.* 2005; 23:7794. [PubMed: 16172456]
12. (a) Wang AZ, Langer R, Farokhzad OC. *Annu Rev Med.* 2012; 63:185. [PubMed: 21888516] (b) Petros RA, DeSimone JM. *Nat Rev Drug Disc.* 2010; 9:615.(c) Caron WP, Morgan KP, Zamboni BA, Zamboni WC. *Clin Cancer Res.* 2013; 19:3309. [PubMed: 23620407]
13. Hrkach J, Von Hoff D, Mukkaram Ali M, Andrianova E, Auer J, Campbell T, De Witt D, Figa M, Figueiredo M, Horhota A, Low S, McDonnell K, Peeke E, Retnarajan B, Sabnis A, Schnipper E, Song JJ, Song YH, Summa J, Tompsett D, Troiano G, Van Geen Hoven T, Wright J, LoRusso P, Kantoff PW, Bander NH, Sweeney C, Farokhzad OC, Langer R, Zale S. *Sci Transl Med.* 2012; 4:12839.
14. (a) Batist G, Gelmon Ka, Chi KN, Miller WH, Chia SKL, Mayer LD, Swenson CE, Janoff AS, Louie AC. *Clin Cancer Res.* 2009; 15:692. [PubMed: 19147776] (b) Svenson S, Wolfgang M, Hwang J, Ryan J, Eliasof S. *J Controlled Release.* 2011; 153:49.
15. (a) Rolland JP, Maynor BW, Euliss LE, Exner AE, Denison GM, DeSimone JM. *J Am Chem Soc.* 2005; 127:10096. [PubMed: 16011375] (b) Chu KS, Schorzman AN, Finnis MC, Bowerman CJ, Peng L, Luft JC, Madden AJ, Wang AZ, Zamboni WC, DeSimone JM. *Biomaterials.* 2013; 34:8424. [PubMed: 23899444] (c) Chu KS, Finnis MC, Schorzman AN, Kuijter JL, Luft JC, Bowerman CJ, Napier ME, Haroon ZA, Zamboni WC, Desimone JM. *Nano Lett.* 2014; 14:1472. [PubMed: 24552251] (d) Gharpure KM, Chu KS, Bowerman C, Miyake T, Pradeep S, Mangala LS, Han H-D, Rupaimoole R, Armaiz-Pena GN, Rahhal TB, Wu SY, Luft C, Napier ME, Lopez-Berestein G, Desimone JM, Sood AK. *Mol Cancer Ther.* 2014
16. Summary methods for synthesis of unsymmetrical dialkylureas:(a) Ozaki S. *Chem Rev.* 1972; 72:457.(a) Gallou I, Eriksson M, Zeng X, Senanayake C, Farina V. *J Org Chem.* 2005; 70:6960. [PubMed: 16095326] (b) Matsumura Y, Satoh Y, Onomura O, Maki T. *J Org Chem.* 2000; 65:1549. [PubMed: 10814121] (c) Gastaldi S, Weinreb SM, Stien D. *J Org Chem.* 2000; 65:3239. [PubMed: 10814225] (d) Han C, Porco JA. *Org Lett.* 2007; 9:1517. [PubMed: 17358074] (e) Liu Q, Luedtke NW, Tor Y. *Tetrahedron Lett.* 2001; 42:1445.(f) Peterson SL, Stucka SM, Dinsmore C. *J Org Lett.* 2010; 12:1340.(g) Dubé P, Nathel NFF, Vetelino M, Couturier M, Aboussafy CL, Pichette S, Jorgensen ML, Hardink M. *Org Lett.* 2009; 11:5622. [PubMed: 19908883]
17. (a) Tsujimoto T, Nishikawa T, Urabe D, Isobe M. *Synlett.* 2005; 433(b) Knapp S, Yu Y. *Org Lett.* 2007; 9:1359. [PubMed: 17338541] (c) Haussener TJ, Looper RE. *Org Lett.* 2012; 14:3632. [PubMed: 22758908] (d) Matsumoto N, Tsujimoto T, Nakazaki A, Isobe M, Nishikawa T. *RSC Adv.* 2012; 2:9448.(e) Malinowski JT, McCarver SJ, Johnson JS. *Org Lett.* 2012; 14:2878. [PubMed: 22617016]
18. (a) Hanessian S, Vakiti RR, Dorich S, Banerjee S, Lecomte F, Del Valle JR, Zhang J, Deschênes-Simard B. *Angew Chem, Int Ed.* 2011; 50:3497.(b) Hanessian S, Vakiti R, Dorich S, Banerjee S, Deschênes-Simard B. *J Org Chem.* 2012; 77:9458. [PubMed: 23083207]
19. Hanessian S, Vakiti RR, Chattopadhyay AK, Dorich S, Lavallée C. *Bioorg Med Chem.* 2013; 21:1775. [PubMed: 23434136]
20. (a) Malinowski JT, Sharpe RJ, Johnson JS. *Science.* 2013; 340:180. [PubMed: 23580525] (b) Sharpe RJ, Malinowski JT, Johnson JS. *J Am Chem Soc.* 2013; 135:17990. [PubMed: 24245656]
21. In these cases, the product was identified as nucleophile addition followed by Payne rearrangement of the resulting epoxy-alcohol.
22. (a) Weller DD, Rinehart KL Jr. *J Am Chem Soc.* 1978; 100:6757.(b) Rinehart KL Jr, Potgieter M. *J Am Chem Soc.* 1981; 103:2099.
23. Waring MJ. *Expert Opin Drug Discov.* 2010; 5:235. [PubMed: 22823020]
24. Chu KS, Hasan W, Rawal S, Walsh MD, Enlow EM, Luft JC, Bridges AS, Kuijter JL, Napier ME, Zamboni WC, DeSimone JM. *Nanomedicine.* 2013; 9:686. [PubMed: 23219874]
25. See Table S1, Supplementary data.
26. See Figure S1, Supplementary data.

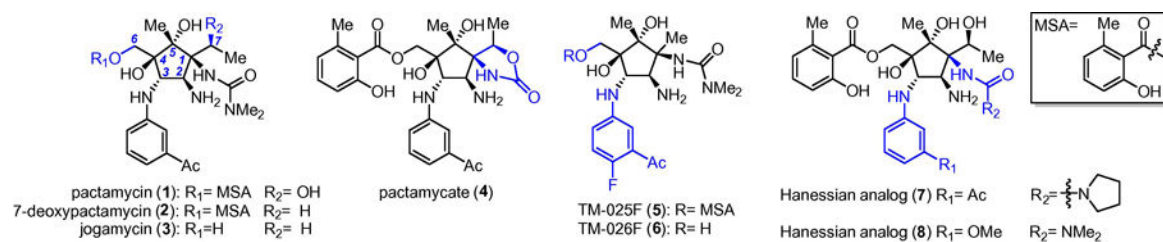


Figure 1.

Structures of pactamycin (1) and natural, synthetic, and biosynthetic congeners.

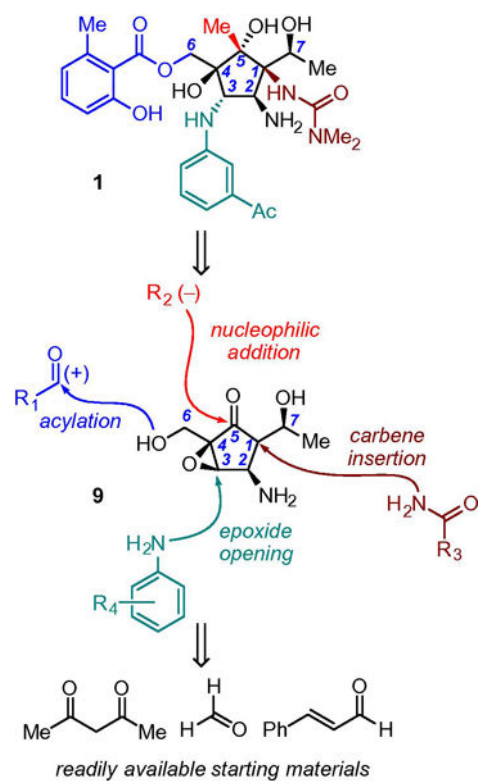


Figure 2.
Synthon analysis of **1** showing key branch points for structural derivatization.

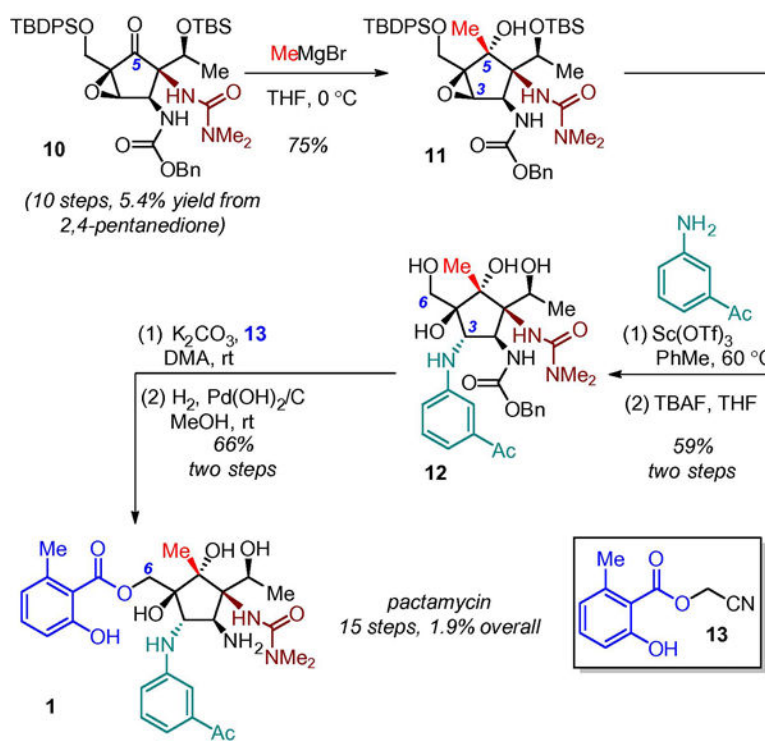


Figure 3.
Pactamycin: endgame strategy and synthesis completion.

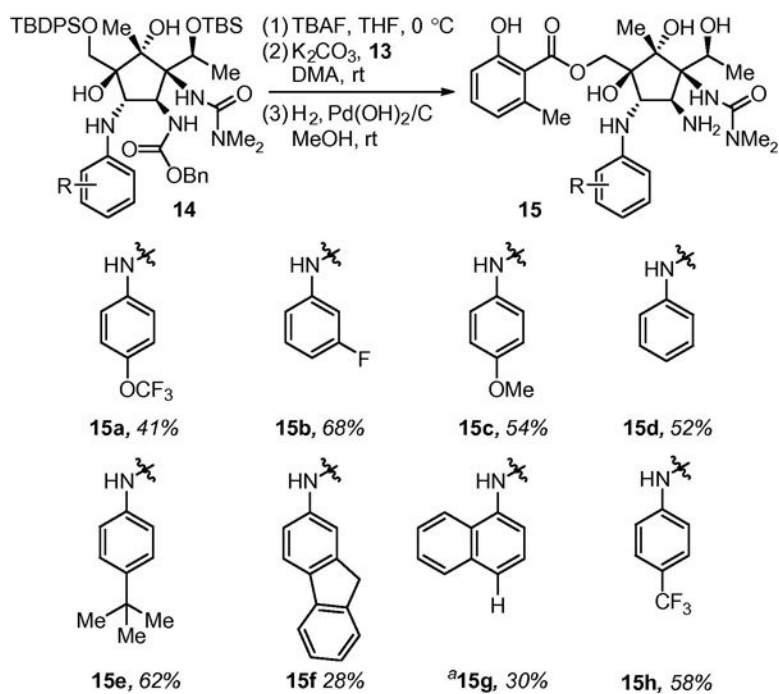
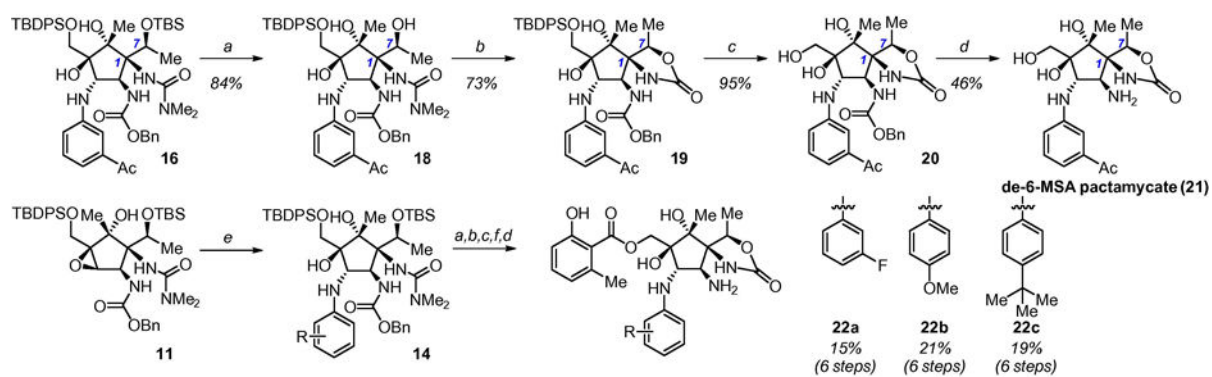


Figure 4. Synthesis of C3 aniline pactamycin derivatives. ^aHydrogenation of the of bromide functionality was observed.

**Figure 5.**

Preparation of de-6-MSA pactamycate and pactamycate analogs. Conditions: (a) oxone, CH₃CN/H₂O (9:1), rt; (b) NH₄Cl, MeOH/H₂O (8:1), 85 °C; (c) TBAF, THF, 0 °C; (d) H₂ (1 atm), Pd(OH)₂/C (0.5 mass equiv), MeOH, rt; (e) aniline (10 equiv), Sc(OTf)₃ (50 mol %), PhMe, 50 °C; (f) K₂CO₃, **13**, DMA, rt.

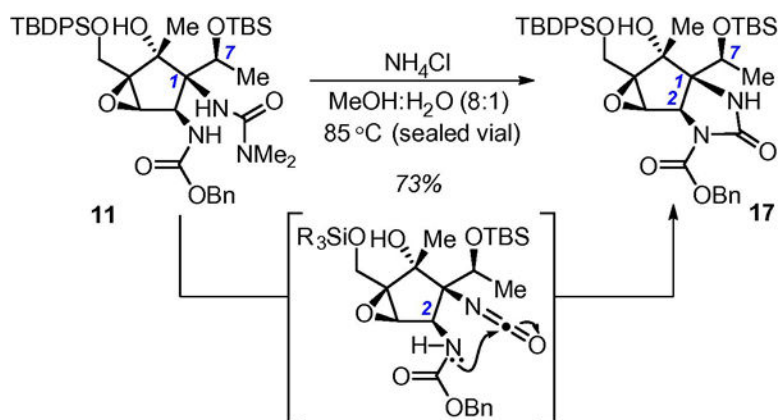
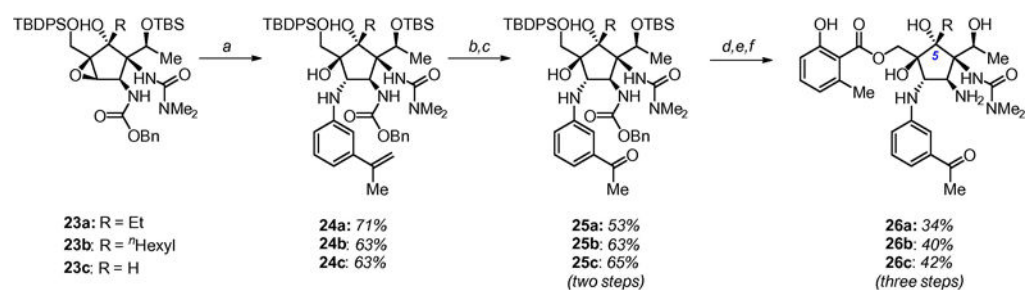


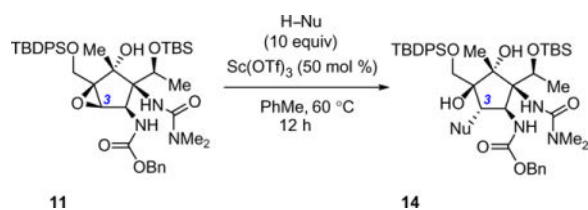
Figure 6.
Failed isocyanate formation/trapping strategy from **11**.

**Figure 7.**

Preparation of C5 pactamycin analogs. Conditions: (a) *m*-propenylaniline (10 equiv), Sc(OTf)₃ (50 mol %), C₇H₈, 50 °C; (b) OsO₄ (10 mol %), NMO (5 equiv), THF/acetone/H₂O (5:5:1), 0 °C–rt; (c) NaIO₄ (3.5 equiv), THF/H₂O (1:1), rt; (d) TBAF, THF, 0 °C; (e) K₂CO₃, **13**, DMA, rt; (f) H₂ (1 atm), Pd(OH)₂/C (0.5 mass equiv), MeOH, rt.

Table 1

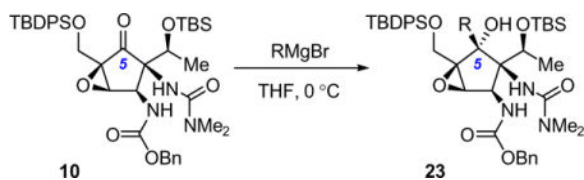
Addition of substituted anilines and other nitrogen nucleophiles to epoxide 11



Entry	H-Nu	Product	% Yield ^a
1		14a	83
2		14b	43
3		14c	95
4		14d	71
5		14e	86
6	2-Fluorenyl aniline	14f	59
7		14g	87
8		14h	47
9		–	<i>_b</i>
10	BnNH ₂	–	<i>_c</i>
11	NaN ₃	–	<i>_d</i>

^a Isolated yield.^b TBS deprotection was observed as the sole product.^c No reaction was observed.^d Conditions: NaN₃ (1.1 equiv), oxone (0.5 equiv), CH₃CN/H₂O (9:1), rt; only TBS deprotection was observed in this reaction.

Table 2

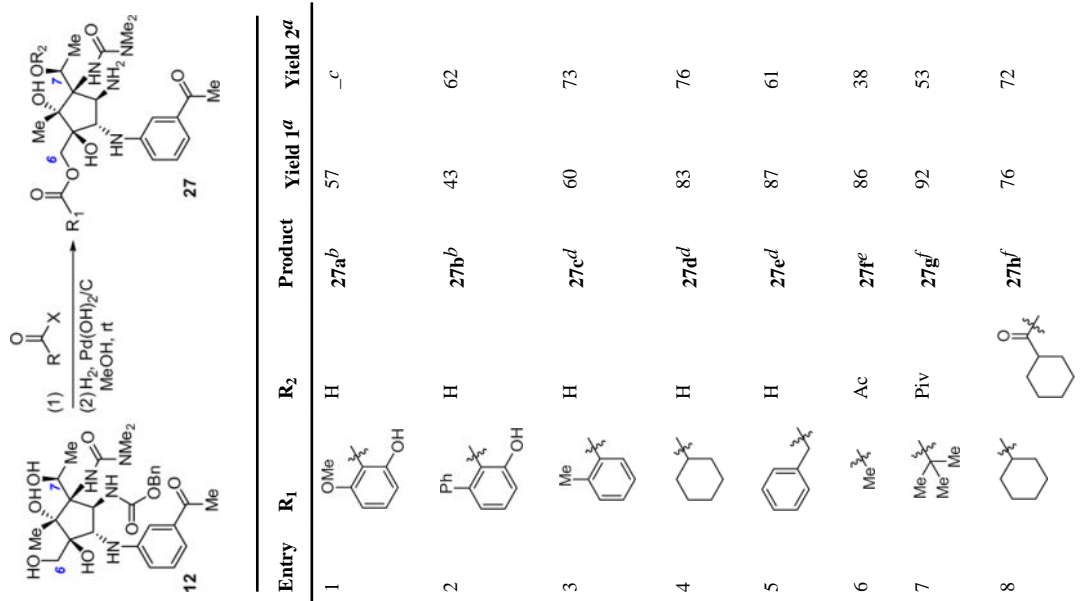
Addition of nucleophiles to ketone **10**^a

Entry	R	Product	% Yield ^b
1	Et	23a	75
2	ⁿ Hexyl	23b	73
3		—	43 ^b
4		—	— ^c
5		—	— ^c
6		—	— ^d
7		—	— ^d
8	PhCH ₂	—	— ^e
9	H	23c	88 ^f

^a Isolated yields.^b Product could not be elaborated further.^c No reaction was observed.^d Undesired side products isolated.^e Complex mixture.^f Conditions: NaBH₄, MeOH, -45 °C.

Table 3

Functionalization of C6 (C7) alcohols



Author Manuscript

Author Manuscript

Author Manuscript

Author Manuscript

^d Isolated yields.

^b X = OCH₂CN; conditions: K₂CO₃, DMA, rt.

^c Only decomposition was observed.

^d X = Cl; conditions: 2,4,6-collidine, CH₂Cl₂, -78 °C to rt.

^e X = OAc; conditions: NEt₃, DMAP (10 mol %), CH₂Cl₂, 0 °C–rt.

^f X = Cl; conditions: NEt₃, DMAP (10 mol%), CH₂Cl₂, 0°C–rt. See Supporting information for details on electrophile preparation.

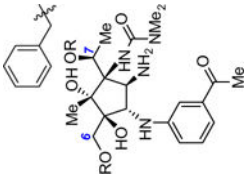
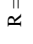
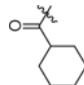
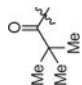
Table 4

Biological examination of pactamycin and synthetic analogs^a

Entry	Structure	Code number	A549 EC ₅₀ (lung cancer)	MDA-MB-231 EC ₅₀ (breast cancer)	SK-OV-3 EC ₅₀ (ovarian cancer)	MRC-5 EC ₅₀ (human lung fibroblast)
1		1	160 nM	124 nM	129 nM	53 nM
2		28	11.8 μM	10.4 μM	12 μM	n.t. ^b
3		<i>ent</i> -(1)	2.1 μM	1.2 μM	1.6 μM	933 nM
4		15a	800 nM	659 nM	1.4 μM	380 nM
5		15b	141 nM	556 nM	434 nM	314 nM
6		15c	1 μM	n.t. ^b	600 nM	582 nM

Entry	Structure	Code number	A549 EC ₅₀ (lung cancer)	MDA-MB-231 EC ₅₀ (breast cancer)	SK-OV-3 EC ₅₀ (ovarian cancer)	MRC-5 EC ₅₀ (human lung fibroblast)
7		15d	777 nM	4 μM	4 μM	682 nM
8		15e	884 nM	3.3 μM	1.6 μM	2326 nM
9		15f	324 nM	376 nM	145 nM	431 nM
10		15g	2.21 μM	1.84 μM	2.44 μM	860 nM
11		15h	760 nM	800 nM	436 nM	366 nM
12		21	6 μM	n.t. ^b	3.8 μM	2933 nM
13		22a	n.t. ^b	n.t. ^b	n.t. ^b	n.t. ^b
14		22b	n.t. ^b	n.t. ^b	n.t. ^b	n.t. ^b
15		22c	n.t. ^b	n.t. ^b	n.t. ^b	n.t. ^b

Entry	Structure	Code number	A549 EC ₅₀ (lung cancer)	MDA-MB-231 EC ₅₀ (breast cancer)	SK-OV-3 EC ₅₀ (ovarian cancer)	MRC-5 EC ₅₀ (human lung fibroblast)
16		26a	n.t. ^b	n.t. ^b	n.t. ^b	2063 nM
17		26b	n.t. ^b	n.t. ^b	n.t. ^b	10.9 μM
18		26c	32 nM	50 nM	7 nM	6.5 nM
19		29	83 nM	356 nM	91 nM	49 nM
20		27b	88 nM	203 nM	103 nM	129 nM
21		27c	114 nM	79 nM	80 nM	105 nM
22		27d	118 nM	300 nM	75 nM	100 nM

Entry	Structure	Code number	A549 EC ₅₀ (lung cancer)	MDA-MB-231 EC ₅₀ (breast cancer)	SK-OV-3 EC ₅₀ (ovarian cancer)	MRC-5 EC ₅₀ (human lung fibroblast)
23		27e	194 nM	352 nM	436 nM	366 nM
24	 R = Ac	27f	137 nM	458 nM	123 nM	132 nM
25		27h	175 nM	1.93 μM	86 nM	396 nM
26		27g	588 nM	2.44 μM	593 nM	778 nM

^a Assays were carried out as triplicates.

^b Not toxic.

Table 5

Summary GI₅₀ values from NCI-60 cell line screening^a

GI ₅₀ (μM)	1 ^b	(ent)-1	26c	27c	15f	27f
MOLT-4	<0.10	1.19	0.046	0.12	0.78	0.33
NCI-H322M	0.12	3.72	0.016	0.33	1.07	0.48
HCT-15	0.03	20.0	0.16	0.65	1.46	10.2
SNB-19	<0.10	3.07	0.52	0.19	1.40	0.57
M14	0.12	3.01	0.10	0.19	0.88	0.68
OVCAR-3	<0.10	2.50	0.041	0.20	0.73	0.53
RXF 393	<0.10	1.50	0.064	0.12	0.61	0.61
DU-145	<0.01	7.26	0.15	0.26	1.37	0.34
MCF7	<0.01	2.04	0.051	0.17	0.73	7.31

^aData obtained from NCI-60 screening. See Supporting information for comprehensive results. MOLT-4, leukemia cell line; NCI-H322 M, nonsmall-cell lung cancer cell line; HCT-15, colon cancer cell line; SNB-19, CNS tumor cell lines; M14, melanoma; OVCAR-3, ovarian cancer cell line; RFX 393, renal cancer cell line; DU-145, prostate cancer cell line; MCF7, breast cancer cell line.

^bData can be accessed from the CAS: 23668-11-3 at the following website: <http://ntp.cancer.gov/dtpstandard/dtwindex/index.jsp>.

Table 6Cell-based assay comparison for compounds **1**, **15e**, **26c** and NP counterparts^a

Compound	A549 EC ₅₀ (nM)	MDA-MB-231 EC ₅₀	MRC-5 EC ₅₀
1	160	124 nM	53 nM
NP-1	52	117 nM	52 nM
15e	884	3.3 μM	2.3 μM
NP-15e	693	5.5 μM	1.8 μM
26c	32	50 nM	6.5 nM
NP-26c	6.5	724 nM	18 nM

^a Assays were carried out as triplicates

Author Manuscript

Author Manuscript

Author Manuscript

Author Manuscript